Primljen / Received: 11.9.2022.
Ispravljen / Corrected: 17.5.2023.
Prihvaćen / Accepted: 18.1.2024.
Dostupno online / Available online: 10.2.2024.

Influence of pore structure characteristics on the strength of aeolian sand concrete

Authors:

[1]Prof.. **Huimei Zhang**
zhanghuimei68@163.com

[2]**Shihang Zheng**, MCE
zhengsh2022@163.com
Corresponding author

[3]**Panyuan Jing**, MCE
jpanyuan@163.com

[1]**Chao Yuan** PhD. CE
yuanchao828@163.com

[4]Prof.. **Yugen Li**
liyugen@yulinu.edu.cn

[1] University of Science and Technology, Xian, China
Department of Mechanics
[2] University of Science and Technology, Xian, China
Collage of Architecture and Civil Engineering
[3] No.1 Bureau of China Metallurgical Geology Bureau, China
[4] Yulin University, China
School of Architecture Engineering

Professional paper

Huimei Zhang, Shihang Zheng, Panyuan Jing, Chao Yuan, Yugen Li

Influence of pore structure characteristics on the strength of aeolian sand concrete

To investigate the influence of the pore structure characteristics of aeolian sand concrete on the mechanical properties, macroscopic mechanical tests of aeolian sand concrete were performed under different conditions, and the influences of the water-cement ratio, sand ratio, and aeolian sand replacement rate on the compressive strength were analysed. The internal microscopic pore structure was characterised using scanning electron microscopy and nuclear magnetic resonance. The impact of pore structure parameters on compressive strength was determined by the grey relational entropy, and a pore structure-strength model was established.

Key words:
aeolian sand concrete, mechanical property, pore structure, function model

Stručni rad

Huimei Zhang, Shihang Zheng, Panyuan Jing, Chao Yuan, Yugen Li

Utjecaj strukture pora na čvrstoću betona od eolskog pijeska

Kako bi se istražio utjecaj karakteristika strukture pora betona od eolskog pijeska na mehanička svojstva, provedena su makroskopska mehanička ispitivanja betona od eolskog pijeska pod različitim uvjetima, a analizirani su i utjecaj vodocementnog omjera, te udjela pijeska i stope zamjene eolskog pijeska na tlačnu čvrstoću. Unutarnja mikroskopska struktura pora ispitana je pomoću skenirajuće elektronske mikroskopije i nuklearne magnetske rezonancije. Utjecaj parametara strukture pora na tlačnu čvrstoću određen je sivom relacijskom analizom, te je utvrđen model čvrstoće i strukture pora.

Ključne riječi:
beton od eolskog pijeska, mehanička svojstva, struktura pora, model funkcije

1. Introduction

With the acceleration of urbanisation and the increasing scale of infrastructure construction in China. As the main material for infrastructure construction, the demand for concrete is increasing; therefore, the demand for natural river sand as an ingredient shows a significant upward trend. The contradiction between the supply and demand of construction sand resources has become a major factor restricting infrastructure construction [1]. The desert area in China is 71.29 million km^2, accounting for 7.4 % of the country's total area, with abundant aeolian sand resources [2]. The utilisation of aeolian sand as fine aggregates instead of river sand to prepare concrete cannot only solve the increasingly serious problem of desertification but also provide a solution to the shortage of construction materials, thereby achieving win–win results.

Aeolian sand concrete is a type of concrete in which aeolian sand partially or completely replaces natural river sand as a fine aggregate. Recently, researchers have studied aeolian sand from different angles but have mainly focused on its engineering characteristics and used it as a raw material to mix concrete. Benabed et al. [3] utilised ultra-fine sand to prepare a self-compacting mortar, and Padmakumar et al. [4], Jiang et al. [5] and Luo et al. [6] prepared concrete using aeolian sand as a fine aggregate and found that aeolian sand can be effectively used as a substitute material for concrete and mortar fine aggregates. Li et al. [7, 8], Dong et al. [9], and Al-Harthy et al. [10] used aeolian sand to replace river sand to prepare concrete and found that the slump rate and strength of the concrete first increased and then decreased with an increase in the aeolian sand content. However, Guettalla [11] and El-Sayed et al. [12] concluded that the strength of concrete decreases with an increase in aeolian sand content, which means that aeolian sand only has negative effects on the technical properties of concrete. The conclusions listed above can be attributed to the obvious regional characteristics of aeolian sand; the compositions of grains and minerals are distinct in different deserts or even in different sections of the same desert.

Concrete is a multiphase heterogeneous composite material with a complex structure. After hardening, many pores of different sizes and shapes are produced in concrete, which affect its strength [13]. Gao et al. [14] used the grey correlation degree and multiple linear regression analysis to obtain the relationship between the pore size distribution and strength of mortar and established a multiple linear regression equation. Bu et al. [15] obtained the porosity and pore distribution of concrete using the mercury intrusion method and established a statistical model for the compressive strength and pore structure characteristics. Dong et al. [16] studied the influence mechanism of pore characteristics on the strength of aeolian sand concrete and found that the correlation between less harmful pores and 28 days compressive strength was the highest. Bai et al. [17] conducted a gray correlation analysis and found that the most important microstructural factor affecting the durability of aeolian sand concrete was the relative proportion of harmful and harmless pores. Liu et al. [18, 19] analysed the pore distribution of aeolian sand concrete using the grey entropy correlation degree and established a grey model for the ratio of compressive strength to pore radius. However, aeolian sand can alter the interface transition zone structure and porosity of materials when added to make aeolian sand owing to its particle gradation and water absorption characteristics, which leads to differences from ordinary concrete in terms of basic mechanical properties, and the available research results regarding the relationship between the pore structure characteristics and the strength of aeolian sand concrete are still insufficient, especially considering that the change in the harmless pore ratio has hardly been reported.

In summary, this study selected different water-cement ratios (0.42, 0.45, and 0.48), sand ratios (30 %, 32 %, and 35 %), and aeolian sand replacement rates (0 %, 20 %, 40 %, 60 %, 80 %, and 100 %) to prepare aeolian sand concrete, and the pore structure characteristics of the different factors of aeolian sand concrete were analysed using scanning electron microscopy (SEM) and NMR. The relationship between mechanical properties and pore structure was studied, and a pore structure-strength relationship suitable for aeolian sand concrete was established.

2. Materials and methods

2.1. Test materials and mix proportion

P.O. 42.5 ordinary Portland cement can be used as cement. Table 1 lists the physical properties of cement. Fine aggregates include river sand and aeolian sand, which can be obtained from the Mu Us Desert in China, and river sand is medium sand. A comparison of the physical properties is presented in Table

Table 1. Main physical properties of cement

Density [kg/m^3]	**Initial setting time** [min]	**Final setting time** [min]	**Compressive strength** [MPa]		**Flexural strength** [MPa]	
			3 days	28 days	3 days	28 days
3151	145	210	24.1	47.3	5.0	8.6

Table 2. Main physical properties of the sand

Sand name	**Bulk density** [kg/m^3]	**Apparent density** [kg/m^3]	**Fineness modulus**	**Water content** [%]	**Soil content** [%]
River sand	1556	2590	2.64	0.3	2
Aeolian sand	1564	2610	0.8	0.5	1.5

Table 3. Main physical properties of the coarse aggregate

Particle size [mm]	**Bulk density** [kg/m³]	**Apparent density** [kg/m³]	**Soil content** [%]
5-20	1652	2640	2.6

Table 4. Concrete mixture proportions

Samples	**Water** [kg/m³]	**Cement** [kg/m³]	**River sand** [kg/m³]	**Aeolian sand** [kg/m³]	**Fly ash** [kg/m³]	**Stone** [kg/m³]
A-1	190	407	450	112	45	1196
A-2	190	380	458	114	42	1216
A-3	190	357	464	116	39	1234
B-1	190	407	422	105	45	1231
B-2	190	407	450	112	45	1196
B-3	190	407	492	123	45	1143
C-1	190	407	562	0	45	1196
C-2	190	407	450	112	45	1196
C-3	190	407	338	224	45	1196
C-4	190	407	226	336	45	1196
C-5	190	407	114	448	45	1196
C-6	190	407	0	562	45	1196

Note: A-1, A-2 and A-3 indicate that the water–cement ratios of 0.42, 0.45, and 0.48, respectively. B-1, B-2 and B-3 indicate that the sand ratios of 30 %, 32 %, and 35 %, respectively. C-1, C-2, C-3, C-4, C-5 and C-6 indicate that the replacement rates are 0 %, 20 %, 40 %, 60 %, 80 % i 100 %.

2 and the gradation curves are shown in Fig. 1. The coarse aggregate was constantly graded crushed stone, and its main physical properties are listed in Table 3. The fly ash was grade II with a specific surface area of 352 m²/kg and a density of 2150 kg/m³. Ordinary tap water was used.

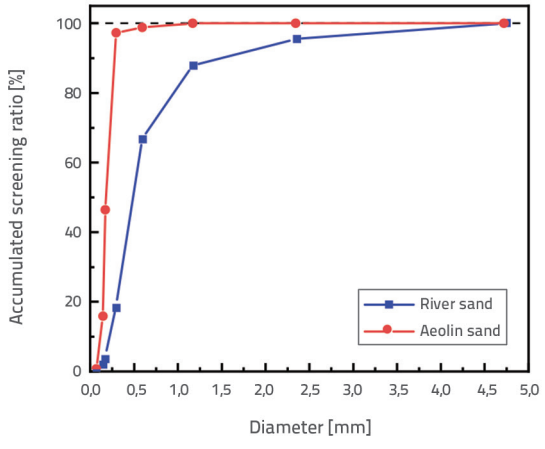

Figure 1. Grading curve of sand for test

This study referred to the code for mix proportion design of ordinary concrete (JGJ55-2011) [20]. The single factor control variable method was used to set different water–cement ratio (sand ratio was 32 %, aeolian sand replacement rate was 20 %, water–cement ratio was 0.42, 0.45, 0.48), sand ratio (water–cement ratio was 0.42, aeolian sand replacement rate was 20 %, sand ratio was 30 %, 32 %, 35 %) and aeolian sand replacement rate (water–cement ratio was 0.42, sand ratio was 32 %, aeolian sand replacement rate was 0 %, 20 %, 40 %, 60 %, 80 %, 100 %). A total of 12 groups of mix ratios were set to prepare aeolian sand concrete with strength grade C40. The specific mix proportions are listed in Table 4.

2.2. Test methods

A standard specimen preparation method based on the mechanical properties was used [21]. Six groups of cube samples with dimensions of 100 × 100 × 100 mm were prepared for each mix proportion; five groups were used for compressive strength, and one group was used to prepare nuclear magnetic resonance samples, with three parallel specimens in each group.

The strength test used a microcomputer electro-hydraulic pressure-testing machine YAW-2000B, and specimens with different curing ages (3, 7, 14, 21, and 28 days) were tested. The corresponding loading rates were 0.50 MPa/s. The NMR test used the MacroMR12-150H-I Nuclear Magnetic resonance (NMR) tester. Before the test, concrete with a curing age of 28 d was sampled using a diamond core machine. The drill size was Ø50 mm in diameter and H100 mm in height. The concrete specimens were subjected to vacuum saturation for 24 h. Porosity and pore structure characteristics were measured using NMR. SEM employed the Zeiss Ø300 field-emission scanning electron microscope. Before the test, a size of approximately 15 × 15 × 5 mm was cut from the centre of the NMR test sample. The structure of the ITZ was examined using SEM.

3. Influence of various factors on compressive strength

3.1. Test results and analysis of compressive strength

A uniaxial compression test of aeolian sand concrete was conducted, and Fig. 2 presents the relationship between the strength of aeolian sand concrete and the curing age under different conditions. The figure illustrates that the development of concrete strength follows a similar pattern, gradually increasing with curing age. This rate of increase is initially slow but then becomes faster, aligning with the general pattern of concrete development. During the initial stage of concrete hardening, the cement hydration reaction occurs rapidly, resulting in a rapid increase in the strength. However, in the later stage of curing, the hydration reaction stabilised, leading to a slower strength growth rate.

As shown in Fig. 2.a, with an increase in the curing age, the compressive strength of aeolian sand concrete increases gradually. When the curing age is 0–7 days, the strength increase rate is faster, and the strength increase rate with the increase of water–cement ratio are 5.3, 5.11, and 4.98 MPa/day. When the curing age is 21–28 days, the strength development is slowest and the strength increase rates are 0.41, 0.24, and 0.14 MPa/d. As the water–cement ratio increased, the strength of the aeolian sand concrete gradually decreased at the same curing age. After the curing period ended, the concrete strength reached its maximum value of 49.6 MPa when the water–cement ratio was 0.42, representing a 7.5 % increase compared to a water–cement ratio of 0.45, and an 11.8 % increase compared to a water–cement ratio of 0.48.

It can be seen from Fig. 2.b that with an increase in the curing age, the growth rate shows a trend of first being slow and then fast. Moreover, the early strength difference of aeolian sand concrete is small under different sand ratios, and the main influence is observed in the late strength development. When the curing age is 0–7 days, the strength increase rate is faster, and the strength increases with the increase of sand ratio are 4.85, 5.21, and 4.6 MPa/day, respectively. When the curing age is 21–28 days, the strength increase rate is slowest, and the strength increase rates are 0.36, 0.3, and 0.32 MPa/day. As the sand ratio increased, the concrete strength initially increased and subsequently decreased at the same curing age. After curing to 28 d, the compressive strength of concrete reaches the maximum value of 49.6 MPa when the sand ratio is 32 %, representing 6.2 % increase compared to a sand ratio is 30 %, and representing 8.8 % increase compared to a sand ratio is 35 %.

It can be seen from Fig. 2.c that the compressive strength development exhibits a pattern of 'fast first and then slow' with an increase in curing age, and the compressive strength of 28 d for each replacement rate meets the configuration requirements of C40 concrete, indicating the feasibility of using aeolian sand as a substitute for river sand. When the curing age is 0–7 days, the strength increase rate is faster, the strength increase rate with the increase of replacement rate are 5.4, 6.47, 5.84, 5.79, 5.88, and 4.9 MPa/day. When the curing age is 21–28 days, the strength increase rate is slowest, the strength increase rates are 0.27, 0.1, 0.11, 0.08, 0.08, and 0.27 MPa/day. As the aeolian sand replacement rate increased, the concrete strength initially increased and subsequently decreased at the same curing age. After the curing period ended, the strength of concrete at replacement rates of 20 %, 40 %, and 60 % was greater than that at the replacement rate of 0 %. The strength reached its maximum value of 49.6 MPa when the replacement rate was 20 %, representing a 7.36 % increase compared to a replacement rate of 0 %, representing a 4.86 % increase compared to a replacement rate of 40 %, representing a 4.42 % increase compared to a replacement rate of 60 %, representing a 9.25 % increase compared to a replacement rate of 80 %, and representing a 13.24 % increase compared to a replacement rate of 100 %.

3.2. Influence of interface area structure on compressive strength

To analyse the influence of different factors on the microscopic structure of aeolian sand concrete, the microscopic morphology of aeolian sand concrete at 28 d of curing age. Fig. 3 depicts the micromorphology of the interface transition zone and the mechanism of action of the aeolian sand concrete under different factors.

As shown in Fig. 3.a, with an increase in the water–cement ratio, small pores gradually developed into larger pores, resulting in noticeable cracks and pores within the interface transition zone. In general, A-1 had a relatively dense structure with small isolated pores during internal closure. A small number of microcracks

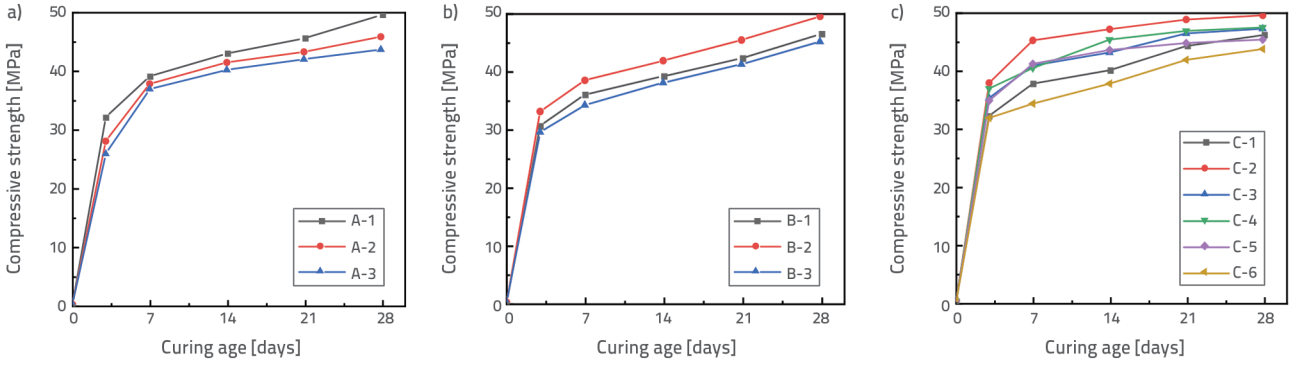

Figure 2. Relationship between the strength and curing age of aeolian sand concrete: a) Water-cement ratio; b) Sand ratio; c) Aeolian sand replacement rate

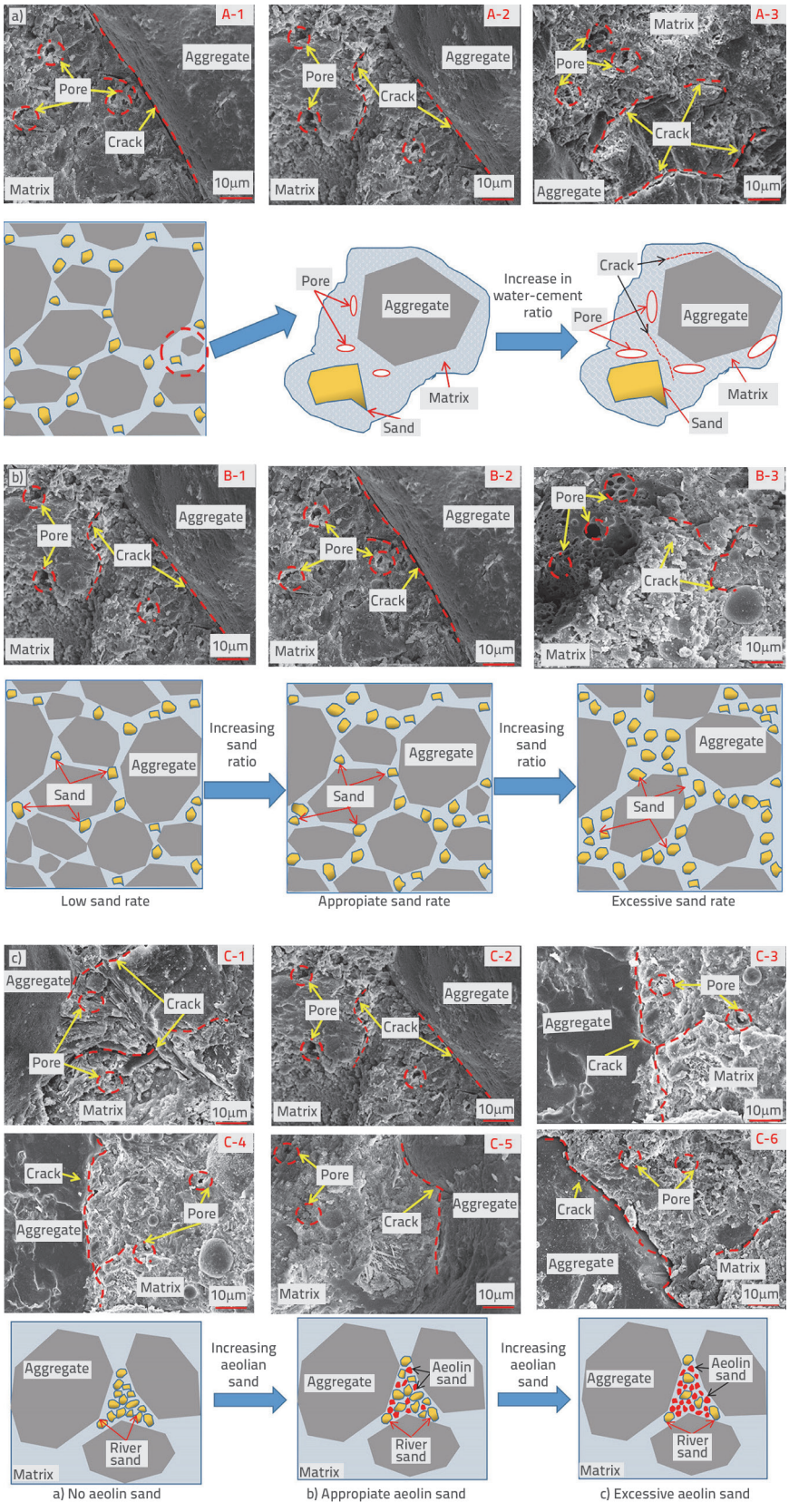

Figure 3. Microstructure and mechanism of aeolian sand concrete: a) Water-cement ratio; b) Sand ratio; c) Aeolian sand replacement rate

were detected, but weak areas were not obvious. By contrast, A-2 exhibits a weak area with differently sized pores and a small number of microcracks caused by hydration shrinkage. A-3 has a relatively loose structure with obvious pores and large staggered cracks visible internally. Combined with the mechanism analysis, the fluidity of the concrete was primarily affected by the consistency of the cement slurry when the water–cement ratio was varied. As the water–cement ratio increased, the consistency of the cement slurry decreased and the fluidity of the concrete mixture increased. This results in the formation of a loose and porous structure in the interfacial transition area, which reduces the bond force between the cement matrix and aggregate surface. This weak structure ultimately leads to a decline in the mechanical properties of the concrete during the later stages of hydration.

It can be seen from Fig. 3.b that with an increase in the sand ratio, the compactness of the structural framework first increases and then decreases, and has pores and cracks. The compactness of B-1 was generally low, with pores and interlaced microcracks. In comparison, B-2 has a relatively higher compactness with closed pores and fewer microcracks. Consequently, it exhibits the highest macroscopic performance strength. B-3 had large visible pores and a relatively loose structure, and the matrix was relatively 'crisp'. Combined with the mechanism analysis, as the sand ratio increased, the specific surface area of the aggregate increased and the thickness of the cement slurry used to wrap the aggregate decreased, resulting in a decrease in the fluidity of the mixture. In addition, a decrease in the number of coarse aggregates further affects the compactness of the structural framework. This weakened the support of the skeleton and reduced the strength of the concrete. When the sand ratio was small, the coarse aggregate content increased, and the pore volume between the aggregates increased, resulting in a decrease in the effective section area of the concrete, and the strength of the concrete was reduced.

As shown in Fig. 3.c, with an increase in the aeolian sand replacement rate, the

compactness of the structure first increased and then loosened, and the internal pores gradually developed into small pores. The compactness of the interface transition zone in C-1 was poor, with noticeable cracks and pores. By contrast, C-2 has a more closely connected interface transition zone, with significantly fewer cracks and pores. C-6 exhibited obvious long cracks and loose cement deposits in the transition zone, resulting in a lower compactness compared to the other concrete groups. Combined with the mechanism analysis, the inclusion of aeolian sand aided in filling the pores between the coarse aggregate and river sand, providing a filling effect that supported the structural framework and refined the pores. This weakens the 'boundary effect' and improves the compactness between the aggregates, resulting in an improved stress distribution of the cement stone under load and enhanced macroscopic performance. However, the round surface of aeolian sand reduces the friction between aggregates, resulting in a decreased need for cement mortar to overcome this friction and enhances the lubrication of the mortar and the strength of concrete. However, owing to the small particle size of aeolian sand, although aeolian sand can reduce the consumption of cement slurry filled with pores, excessive addition can cause insufficient cement mortar to wrap around the aggregates, increasing the friction between the aggregates and ultimately reducing the strength of the concrete.

3.3. Influence of pore structure on compressive strength

Concrete is a multiphase and multilevel composite material [22], and its macro performance is determined by its microstructure. The complexity and uncertainty of the microstructure determines the variability and irregularity of the macrophysical characteristics of a material. Nuclear Magnetic Resonance (NMR) is a nondestructive testing technology that has unique advantages in characterising microscopic pores. According to the nuclear magnetic resonance principle [23, 24], the relaxation time is proportional to the pore size and is affected by the specific surface area of the pores in the material. Assuming that the pores are ideal spheres, the T_2 map can be transformed into the pore-size distribution of the material.

Fig. 4 shows the pore size distribution curves of the aeolian sand concrete with different factors. The curves show the percentage of each pore size in all the pores. The higher the percentage, the greater the number of pores. The starting point of the curve represents the minimum pore size present in concrete, whereas the highest peak value indicates the pore size with the highest proportion in the sample, which is also known as the most probable pore size. It can be seen that the pore size distribution of concrete is primarily concentrated between 0.001–0.1μm and exhibits a 'multi-peak' structure composed of 3-4 peaks. The first peak, which accounted for over 85 % of the distribution, was significantly larger than the other peaks.

It can be seen from Fig 4.a that with an increase in the water–cement ratio, the starting peak position first moves right and then left, indicating an initial increase and then a decrease in the minimum pore size of the material. Similarly, the end peak position moves first to the left and then to the right, indicating that the maximum pore size first decreases and then increases. Additionally, the amplitude of the first peak gradually decreases, indicating a decrease in the proportion of the most probable pore size in the material. In addition, the size of the first peak in the pore-size distribution curve accounted for 92 % when the water–cement ratio was 0.42, and the second and third peaks were relatively small. When the water–cement ratio was 0.45 and 0.48, the size of the first peak accounted for 87 %, and the second and third peaks were relatively large, with a superposition peak phenomenon. This indicates a higher small pore content and a lower large pore content when the water-binder ratio is 0.42.

As shown in Fig. 4.b, with an increase in the sand ratio, the amplitude of the first peak first increased and then decreased. When the sand ratio was 32 %, the amplitude of the first peak was the highest; the proportion of pore size corresponding to the second, third, and fourth peaks was smaller; and the pore size corresponding to the end of the peak was smaller, indicating that the maximum pore size present in the material was smaller at this time. When the sand ratio was 30 %, the pore sizes corresponding to the second and third peaks were larger and the pore size corresponding to the end of the peak was the largest. When the sand ratio was 35 %, the subpeaks began to overlap, indicating that the material had more large pores.

As shown in Fig. 4.c, with an increase in the aeolian sand replacement rate, the starting peak position moved to the left. This is primarily owing to the incorporation of aeolian sand, which increases the density of cement stone in the concrete, resulting in a gradual decrease in the minimum pore size. The proportion of the first peak gradually increased, whereas the proportion of its second peak decreased, indicating that the proportion of small pores increased and the proportion of large pores decreased. When the replacement rate was 0 %, the first peak accounted for

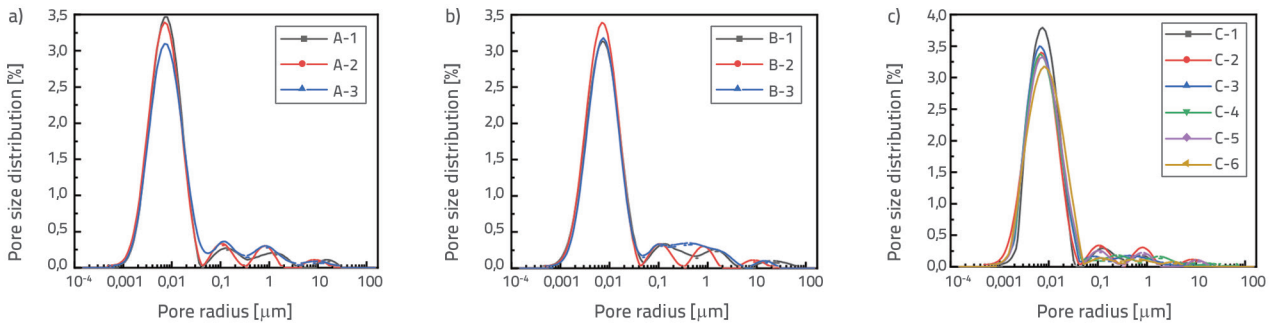

Figure 4. Pore size distribution curves of aeolian sand concrete: a) Water-cement ratio; b) Sand ratio; c) Aeolian sand replacement rate

Table 5. Pore characteristic parameters of aeolian sand concrete

Samples	Total porosity [%]	Minimum pore size [μm]	Maximum pore size [μm]	Most probable pore size [μm]	Average pore size [μm]
A-1	4.72	0.00017	26.44371	0.00732	0.09222
A-2	5.48	0.00098	8.12381	0.00732	0.07173
A-3	5.93	0.00017	42.99101	0.00732	0.12370
B-1	5.39	0.00018	69.89289	0.00683	0.23495
B-2	4.72	0.00017	26.44371	0.00732	0.09222
B-3	5.68	0.00018	28.34479	0.00785	0.13340
C-1	5.41	0.00851	9.33386	0.00785	0.02577
C-2	4.72	0.00017	26.44371	0.00732	0.09222
C-3	5.18	0.00060	24.67014	0.00683	0.035805
C-4	5.08	0.00069	74.91758	0.00683	0.070981
C-5	5.65	0.00060	18.68825	0.00785	0.058362
C-6	6.08	0.00056	5.35618	0.00841	0.019804

93 % of the total peaks, indicating a clear four-peak structure. When the replacement rate was 100 %, the proportion of the first peak increased to 96 %, whereas the second and third peaks merged into lower peaks. This suggests that the addition of aeolian sand is beneficial for converting large pores into small pores and reducing the total number of pores in concrete.

The pore characteristics of concrete are characterised by parameters such as the total porosity, minimum pore size, maximum pore size, most probable pore size, and average pore size, as determined by the pore size distribution curve obtained through nuclear magnetic resonance tests. Table 5 lists the specific parameters used to study the influence of different factors on the pore characteristics of aeolian sand concrete.

It can be seen from Table 5 that with an increase in the water–cement ratio, the porosity increased gradually, the minimum pore size first increased and then decreased, and the maximum and average pore sizes first decreased and then increased. The analysis indicated that as the water–cement ratio increased, the fluidity of the concrete mixture increased. However, the binding water required for cement hydration accounts for approximately 25 % of the total cement quantity. Therefore, additional water was required to achieve the desired level of fluidity. When concrete hardens, the water within the concrete forms bubbles, leading to an increase in local porosity and the formation of a weaker structure. This can reduce the effective section of the resistance of concrete to load, ultimately affecting its mechanical properties.

With an increase in sand ratio, the porosity first decreased and then increased, the minimum pore size remained unchanged, the maximum and average pore sizes first decreased and then increased, and the most probable pore size increased. The analysis indicated that when the sand ratio was small, the number of coarse aggregates increased and the pore volume between the aggregates increased, which reduced the effective cross-sectional area and strength of the concrete. When the sand ratio is appropriate, the internal aggregate of the material exhibits a uniform particle size distribution and good particle gradation, resulting in a closer structural skeleton, reduced porosity, and increased concrete strength. When the sand ratio was high, the specific surface area of the aggregate increased, causing the cement slurry used to encapsulate the aggregate to become thinner and resulting in a decrease in the fluidity of the mixture. Additionally, a reduction in the number of coarse aggregates increases the porosity, which weakens the structure and ultimately decreases the strength of the concrete.

With an increase in the aeolian sand replacement rate, the porosity first decreased and then increased, and the minimum pore size first decreased and then increased. The trends of the maximum and average pore sizes first increased and then decreased, and the most probable pore sizes were relatively close. The analysis indicated that the small particle size of aeolian sand allowed it to fill the pores between coarse aggregates and river sand, thereby improving the compactness between aggregates. The addition of an appropriate amount of aeolian sand improves the aggregate gradation of concrete and makes the particle size between aeolian sand, river sand, and stone approximately satisfy the continuous gradation theory, thus realising the mutual filling of pores between different particle sizes, refining the pores, reducing the pore volume between coarse aggregates, and enhancing the macro performance of concrete. Excessive aeolian sand can exacerbate the 'boundary' effect, leading to the formation of more adjacent loose cement accumulation bodies and local high water cement ratio areas in concrete. This, in turn, increases the porosity and reduces the compactness of the structure, ultimately diminishing the mechanical properties of the concrete.

4. Micro-structure and macroscopic mechanical properties of aeolian sand concrete

4.1. Pore size

As a porous material, the mechanical properties of concrete are influenced by the pore size, that is, the pore structure, and the influence of different pore sizes on the mechanical properties

of concrete varies. According to Academician Wu [25] on the classification standard of pore size in concrete, the pore structure can be divided into harmless pore (d ≤ 20 nm), less harmful pore (20 < d ≤ 50 nm), harmful pore (50 < d ≤ 200 nm), more harmful pore (d > 200 nm). The pore structure in Figure 4 was classified and counted, and its influence on the compressive strength was considered. The results are shown in Figure 5.

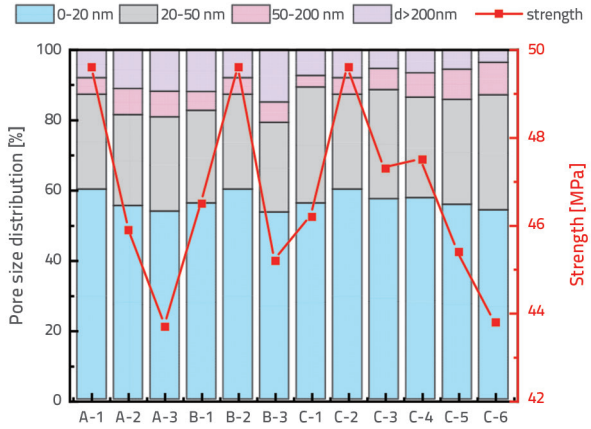

Figure 5. Relationship between pore size proportion and strength

As shown in Figure 5, the contents of harmless and less harmful pores in the pore size classification of aeolian sand concrete under different factors were larger. As the water–cement ratio gradually increases, the strength gradually decreases, which is 7.5 % and 11.8 % lower than that of 0.42. The harmless pore content gradually decreased and was 7.7 % and 10.5 % lower than that of 0.42. The content of less harmful pores first decreased and then increased, and was 4.5 % and 0.6 % lower than that of 0.42, respectively. The porosity of harmful and more harmful pores gradually increased; the number of harmful pores was 59.9 % and 56.9 % higher than that of 0.42, respectively, and the number of multi-hazard pores was 38.5 % and 47.4 % higher than that of 0.42, respectively. An increase in the water–cement ratio results in an increase in the free water content and internal pores within the materials, ultimately decreasing the strength.

As the sand rate gradually increased, the strength first increased and then decreased, increasing by 6.6 % and decreasing by 2.8 % compared with a sand rate of 30 %. The content of harmless pores first increased and then decreased, increasing by 7 % and decreasing by 4.7 %, respectively, compared with the sand rate of 30 %. The content of less harmful pores first increased and then decreased, increasing by 2.6 % and decreasing by 2.9 %, respectively, compared with the sand rate of 30 %. The content of harmful pores first decreased and then increased, decreasing by 12.9 % and increasing by 8.6 %, respectively, compared with the sand rate of 30 %. The content of more harmful pores first decreased and then increased, decreasing by 33 % and increasing by 24.7 %, respectively, compared with the sand rate of 30 %. The difference in sand rate mainly affects the encapsulation and fluidity of concrete, which consequently affects the compactness of the structural skeleton and alters the porosity of the material.

As the aeolian sand replacement rate increased, the strength first increased and then decreased, increasing by 7.4 %, 2.4 %, and 2.8 % and decreasing by 1.7 % and 5.2 %, respectively, compared to the replacement rate of 0 %. The harmless pore content first increased and then decreased, and the range of variation was between 54.15 % and 60.09 %. The content of less harmful pores first decreased and then increased, and the content was 27.22 %–33.21 %. The content of harmful pores gradually increased from 3.3 % to 9.28 %. The content of more harmful pores decreased in a wave-like manner, with a content of 3.6 %–8.03 %, showing poor regularity. This is because the aeolian sand particles are round and poorly graded, and the particle size is relatively concentrated, which can fill the pores between the coarse aggregate and river sand and enhance the compactness between the aggregates. Therefore, when the replacement rate of the aeolian sand changed, the pore radius became more concentrated, harmless, and less harmful.

The results In Figure 5 indicate that the content of harmless pores follows a pattern consistent with the development of concrete strength, regardless of other factors. Specifically, an increase in harmless pore content led to an increase in strength, whereas a decrease in harmless pore content resulted in a decrease in strength. Thus, it can be inferred that the harmless pore content plays a significant role in the development of concrete strength.

4.2. Porosity

Porosity is a crucial indicator of the pore structure of porous materials. Porosity is closely related to density and strength of a material. To further investigate the relationship between the macro- and microcharacteristics of aeolian sand concrete with different factors, Figure 6 illustrates the variation law of the strength and porosity of aeolian sand concrete with different factors.

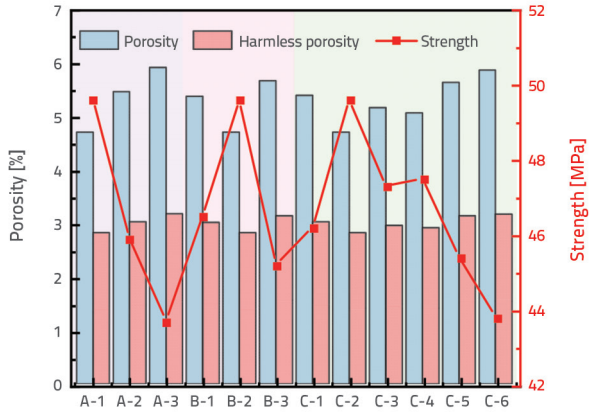

Figure 6. Relationship between porosity and strength

It can be observed from the figure that with an increase in the water-cement ratio, the strength decreases gradually, which is 7.5 % and 11.8 % lower than that of the water-cement ratio of 0.42. The porosity increased gradually and was 16.1 % and 25.6 % higher than that of the water–cement ratios of 0.42. The harmless porosity increases gradually, which are 7.1 % and 12.5 % higher than that of water–cement ratio 0.42. The porosity was

at its minimum, and the strength was at its maximum when the water-cement ratio was 0.42.

With an increase in the sand ratio, the strength first increased and then decreased, increasing by 6.6 % and decreasing by 2.8 %, respectively, compared with a sand ratio of 30 %. The porosity first decreased and then increased, decreasing by 12.5 % and increasing by 5.2 %, respectively, compared with a sand rate of 30 %. The harmless porosity first decreased and then increased, decreasing by 6.2 % and increasing by 4.2 %, respectively, compared with a sand rate of 30 %. The porosity was at its minimum, and the strength was at its maximum when the sand ratio was 32 %.

With an increase in the aeolian sand replacement rate, the strength first increased and then decreased. Compared to the replacement rate of 0 %, the strength increased by 7.4 %, 2.4 %, and 2.8 % and decreased by 1.7 % and 5.2 %, respectively. Compared to the 0 % replacement rate, the porosity first decreased and then increased by 12.7 %, 4.3 %, and 6.1 %, and then increased by 4.4 % and 8.7 %, respectively. Compared to the 0 % replacement rate, the harmless porosity first decreased and then increased by 6.6 %, 2.1 %, and 3.5 %, and then increased by 3.7 % and 4.8 %, respectively. The porosity was at its minimum, and the strength was at its maximum when the replacement rate was 20 %.

Based on the data presented in Fig. 6, it can be observed that there is an inverse relationship between porosity and strength development in concrete. Specifically, the strength increased as the porosity decreased. This suggests that porosity plays a significant role in determining the strength of concrete.

5. Pore structure strength model based on grey correlation entropy analysis

5.1. Grey correlation entropy analysis

The grey correlation entropy analysis method is an important technique for grey models. This helps to prevent errors caused by the local control of the entire system when determining the degree of grey correlation. This method can effectively distinguish the impacts of primary and secondary factors on the entire system [26].

To investigate the influence of the pore structure characteristic parameters of aeolian sand concrete on its compressive strength under different factors, we conducted a grey correlation entropy analysis on the pore structure test data and compressive strength of concrete measured by NMR. The compressive strength was taken as the reference column, and the porosity, minimum pore size, maximum pore size, most probable pore size, average pore size, and proportion of each pore radius interval were used as the comparison sequence to obtain the grey entropy correlation degree between the compressive strength of aeolian sand concrete with different factors and the proportion of pore structure parameters and pore radius interval. Table 6 displays the degree of correlation of grey entropy in aeolian sand concrete with various factors.

The compressive strength of aeolian sand concrete with different factors is affected by various pore structure parameters and the proportion of the pore radius interval. Based on the grey entropy correlation degree, the most influential pore structure parameter is the most probable pore size, followed by porosity, average pore size, maximum pore size, and minimum pore size, whereas the most influential pore radius ratio is harmless pores, followed by less harmful pores, harmful pores, and more harmful pores.

The study found that the degree of grey entropy correlation between the compressive strength of aeolian sand concrete with different factors was the highest, with the proportion of the most probable pore size and harmless pore size. This suggests that the proportion of harmless pores and the most probable pore size have the greatest impact on the compressive strength of concrete. Because the most probable pore size increases, the proportion of the pore radius in harmless pores also increases, resulting in denser concrete and greater compressive strength.

5.2. Establishment of pore structure-strength model

Regression analysis is a statistical method used to examine the linear or non-linear relationship between a dependent variable and one or more independent variables. Regression analysis and prediction are methods used to calculate causal relationships and influencing factors between predicted objects. This method considers all influencing factors of the predicted objects, resulting in smaller errors. In addition, the predicted values can be adjusted based on the corresponding change factors when the system undergoes significant changes, making it suitable for long-term predictions.

Grey theory was used to analyse the correlation between various influencing factors, compressive strength, and the

Table 6. Grey entropy correlation degree of aeolian sand concrete

Parameter	Water-cement ratio	Sand ratio	Replacement rate	Different factors
Minimum pore size	0.975	0.982	0.973	0.971
Maximum pore size	0.948	0.965	0.986	0.979
Most probable pore size	0.990	0.982	0.991	0.992
Average pore size	0.986	0.959	0.987	0.982
Porosity	0.987	0.980	0.989	0.989
Harmless pore	0.989	0.983	0.991	0.993
Less harmful pore	0.987	0.979	0.989	0.987
Harmful pore	0.986	0.978	0.987	0.979
More harmful pore	0.981	0.965	0.988	0.977

Table 7. Dimensionless averaging of aeolian sand concrete with different factors

Samples	Compressive strength [MPa]	The most probable pore size [μm]	The proportion of harmless pores [%]	Harmless porosity [%]
A-1	1.033	1.045	1.026	0.982
A-2	0.955	0.975	0.978	1.047
A-3	0.911	0.974	0.949	1.113
B-1	0.951	0.910	0.991	1.094
B-2	1.013	1.045	1.003	0.969
B-3	0.924	1.045	0.944	1.096
C-1	1.026	1.045	1.026	0.969
C-2	1.102	0.975	1.060	0.874
C-3	1.051	0.910	1.048	0.949
C-4	1.055	0.910	1.018	0.904
C-5	1.008	1.045	1.001	0.988
C-6	0.973	1.120	0.955	1.015

degree of influence of various factors on compressive strength. Additionally, the grey theory was combined with a regression model to construct a compressive strength prediction model based on grey theory regression with processed dimensionless data. The study initially analysed and processed data on different factors using the mean dimensionless method, as presented in Table 7. Based on the correlation degree ranking, a grey theory regression pore structure-strength model was established using the compressive strength of concrete, most probable pore size, proportion of harmless pores, and harmless porosity.

Assuming that the pore structure-strength relationship is:

$$f_c = \alpha + \beta_1 d_p - \beta_2 p_h + \beta_3 n_h \quad (1)$$

In Eq (1), f_c is compressive strength, d_p is the most probable pore size of concrete, p_h is the proportion of harmless pores of concrete, n_h is harmless porosity of concrete, α, β_1, β_2, β_3 are regression parameters.

The expression parameters of the dimensionless pore structure-strength relationship were obtained through regression analysis. These parameters are introduced into Equation (1) to obtain Equation (2).

$$f_c = 1{,}399 + 0{,}237 d_p - 0{,}724 p_h + 0{,}30 n_h \quad (2)$$

The data in Table 5 were used in Equation (2) to obtain the dimensionless compressive strength. The calculated compressive strengths were in good agreement with the test values with a correlation coefficient of $R^2 = 0.996$. The average relative error between the predicted and experimental values of the pore structure-strength model of aeolian sand concrete and the test value was 0.86 %, indicating that the model was highly accurate. The compressive strength can be predicted using the pore structure parameters of the concrete and the proportion of the pore radius interval. The results are presented in Fig. 7.

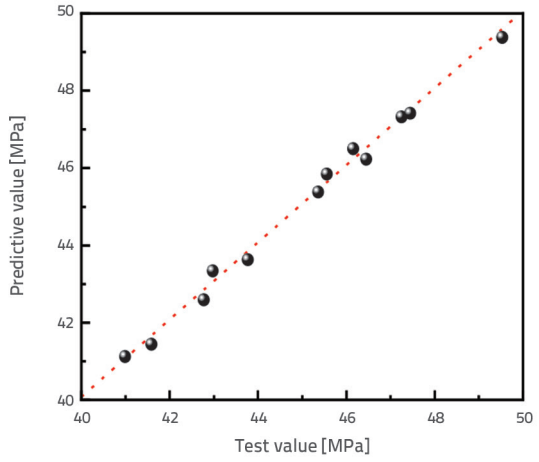

Figure 7. Comparison of model predictive value and test value

6. Conclusion

This paper presents the results of mechanical property, NMR, and SEM tests conducted on aeolian sand concrete under different conditions. The pore structure characteristics of aeolian sand concrete are discussed from both the macro- and micro-perspectives, considering the effects of different factors. The relationship between the mechanical properties and pore structure was analysed using grey correlation entropy. The conclusions are as follows.

- The compressive strength of concrete decreased with an increase in the water–cement ratio and first increased and then decreased with an increase in the sand ratio and aeolian sand replacement rate.
- The pore size distribution curve of the aeolian sand concrete displayed multiple peaks, and the pore size distribution fell within 0.001–0.1 μm range. The main peak amplitude decreased with an increase in the water–cement ratio and aeolian sand replacement rate and first increased and then decreased with an increase in the sand ratio.

- The compressive strength of aeolian sand concrete had the highest correlation with the most probable pore size and proportion of harmless pores, with grey entropy correlations of 0.992 and 0.993, respectively.
- According to the pore structure-strength model, which considers the most probable pore size, proportion of harmless pores, and harmless porosity, the strength of aeolian sand concrete can be accurately predicted, with an average relative error of 0.86 %.

Acknowledgements

The work was supported by the National Natural Science Foundation of China (12172280, 52268047, 51868075); The Key project of Natural Science Foundation of Shaanxi (2020JZ-53); Industry-University-Research Project of Yulin with a Grant No. of 2019-101-6, and the Yulin High-tech Zone Science and Technology Bureau with Grant No. of CXY-2020-10; The youth project of Natural Science Foundation of Shaanxi (2024JC-YBQN-0273).

REFERENCES

[1] Bendixen, M., Best, J., Hackney, C.R., et al: Time is running out for sand, Nature, 571 (2019), pp. 29-31.

[2] Xue, H.J., Shen X.D., Liu Q., et al.: Analysis of the damage to the aeolian sand concrete surfaces caused by wind-sand erosion Journal of Advanced Concrete Technology, 15 (2017), pp. 724-737.

[3] Benabed, B., Azzouz, L., Kadri, E.H., et al: Effect of fine aggregate replacement with desert dune sand on fresh properties and strength of self-compacting mortars, Journal of Adhesion Science and Technology, 28 (2014), pp.2182-2195.

[4] Padmakumar, G., Srinivas, K., Uday, K.V., et al.: Characterisation of aeolian sands from Indian desert, Engineering Geology, (2012), pp. 38-49.

[5] Jiang, J.Y., Feng, T.T., Chu, H.Y., et al.: Quasi-static and dynamic mechanical properties of eco-friendly ultra-high-performance concrete containing aeolian sand, Cement and Concrete Composites (2019). https://doi.org/10.1016/j.cemconcomp.2019.01.011.

[6] Luo, F.J., He, L.F., Pan, Z., et al.: Effect of very fine particles on workability and strength of concrete made with dune sand, Construction and Building Materials, 47 (2013), pp. 131-137.

[7] Li, Y.G., Zhang, H.M., Liu, G.X. et al.: Multi-scale study on mechanical properties and strength prediction of aeolian sand concrete, Construction and Building Materials, 247 (2020), p. 118538.

[8] Li, Y.G., Zhang, H.M., Liu, G.X. et al.: Time-varying compressive strength model of aeolian sand concrete considering the harmful pore ratio variation and heterogeneous nucleation effect, Advances in Civil Engineering, (2019). https://doi.org/10.1155/2019/5485630.

9] Dong, W., Xiao, Y., Su, Ying, et al.: Study on axial compression performance of aeolian sand concrete, Advanced Engineering Sciences, 52 (2020), pp. 86-92.

[10] Al-Harthy, A., Halim, M.A., Taha, R.A., et al., Properties of concrete made with fine dune sand, Construction and Building Materials, 21 (2007), pp. 1803-1808..

[11] Guettala, S., Mezghiche, B.: Compressive strength and hydration with age of cement pastes containing dune sand powder. Construction and Building Materials, 25 (2011), pp. 1263-1269.

[12] Seif, E.S.: Assessing the engineering properties of concrete made with fine dune sands: An experimental study. Arabian Journal of Geosciences, 6 (2013), pp. 857-863.

[13] Lian, C.Q., Zhuge, Y., Beecham, S.: The relationship between porosity and strength for porous concrete, Construction and Building Materials, 25 (2011), pp. 4294-4298.

[14] Gao, H., Zhang, X., Zhang, Y.: Effect of the entrained air void on strength and interfacial transition zone of air-entrained mortar, Journal of Wuhan University of Technology-Mater. Sci. Ed., 30 (2015),pp. 1020-1028.

[15] Bu, J., Tian, Z.: Relationship between pore structure and compressive strength of concrete: experiments and statistical modelling, Sādhanā, 41 (2016), pp. 337-344.

[16] Dong, R.X., Shen, X.D., Liu, Q., et al.: Influence mechanism of pore characteristics of aeolian sand concrete on its strength, Bulletin of Chinese Ceramic Sociery, 38 (2019), pp. 1901-1907.

[17] Bai, J.W., Zhao, Y.R., Shi, J.G. et al.: Cross-scale study on the mechanical properties and frost resistance durability of aeolian sand concrete, KSCE Journal of Civil Engineering, 25 (2021), pp. 4386-4402.

[18] Liu, Q., Shen, X. D., Wei, L. S., et al.: Grey model research based on the pore structure fractal and strength of NMR aeolian sand lightweight aggregate concrete, JOM, 72 (2020), pp. 536-543.

[19] Liu, Q., Shen, X.D., Dong, R.X., et al.: Grey entropy analysis on effect of pore structure on compressive strength of aeolian sand concrete, Transactions of the Chinese Society of Agricultural Engineering, 35 (2019), pp. 108-114.

[20] JGJ 55. 2011. Specifications for the mix proportion design of ordinary concrete. JGJ 55, China Architecture and Building Press, Beijing.

[21] GB/T 50081. 2019. Standard test method for the mechanical properties of ordinary concrete. GB/T 50081; China Architecture and Building Press, Beijing, China.

[22] Xue, H.J., Shen, X.D., Zou, C.X., et al.: Freeze-thaw pore evolution of aeolian sand concrete based on nuclear magnetic resonance Journal of Building Materials, 22 (2019), pp. 199-205

[23] Cui, S.A., Liu, P., Cui, E.Q., et al: Experimental study on mechanical property and pore structure of concrete for shotcrete use in a hot-dry environment of high geothermal tunnels, Construction and Building Materials, 173 (2018), pp. 124-135.

[24] Ji, Y.L., Sun, Z.P., Yang, X. et al.: Assessment and mechanism study of bleeding process in cement paste by 1H low-field NMR, Construction and Building Materials, 100 (2015), pp. 255-261.

[25] Wu, Z.W.: Discussion on the recent development direction of concrete science and technology Journal of the Chinese Ceramic Society, 03 (1979), pp. 262-27

[26] Zhang, M., Yao, X.H., Guan, J.F., et al: Study of concrete strength and pore structure model based on grey relation entropy, Materials, 14 (2021). https://doi.org/10.3390/ma14020432.